RSC Advances

PAPER

View Article Online
View Journal | View Issue

Cite this: *RSC Adv.*, 2021, **11**, 1662

Effects of potassium additives on the combustion characteristics of graphite as a heating source of heat-not-burn tobacco

Chenghao Luo,[a] Dan Li,[a] Long Huang,*[a] Zean Wang,*[bc] Jian Zhang,[b] Hao Liu[b] and Zhaohui Liu[b]

"Heat-not-burn" tobacco with an external heating source is a cleaner alternative to conventional cigarettes due to its lower emission of nicotine, CO and tar in the smoke, and graphite is a promising carbon heating source for a "heat-not-burn" tobacco product yet is not easy to be fired. This work aims to improve the combustion properties of graphite using potassium catalysts. Thermal gravimetric analysis is performed to investigate the combustion properties, and a first-order kinetic model is applied to describe the combustion process. Scanning electron microscopy is used to observe the surface morphology, and the mineral and elemental composition are investigated by powder X-ray diffraction and energy dispersive spectrometry, respectively. The results indicate that the potassium additives can significantly decrease the ignition temperature of the graphite samples by 51–124 °C, and the promotion effects are closely related to the potassium and oxygen content of the additives. Further kinetic analysis implies that K and O can decrease the activation energy required for the oxidation reactions by 45.1% from 194.5 to 106.8 kJ mol^{-1}, thereby improving the graphite combustion. Moreover, potassium can play the role of "O_2 transfer", which can transfer atmospheric oxygen to support graphite combustion. K_2CO_3 is a suitable catalyst for graphite combustion, and the suggested addition amount is 0.88% in weight.

Received 29th October 2020
Accepted 10th December 2020

DOI: 10.1039/d0ra09213d

rsc.li/rsc-advances

Introduction

Direct combustion of conventional cigarettes can produce a significant amount of environmental tobacco smoke, which is posing a great threat to public health.[1] To reduce the amount of pollutants in smoke, new types of alternatives, *i.e.* electronic cigarettes (e-cigarettes) and "heat-not-burn" (HNB) tobacco, are now commercially developed to deliver an aerosol with fewer pollutants than in conventional tobacco smoking.[2,3] A common HNB tobacco product is usually composed of a tobacco stick, a holder, and an external heating system. The tobacco stick is inserted into the holder and heated with an external heating system to deliver the aerosol.[4] Once the tobacco formula is determined, the external heating source, the core part of the external heating system, would become the most significant component for an HNB tobacco product.

Currently, the external heating system generally involves electricity (*i.e.* 'Juul' from JUUL Labs, 'iQos' from Philip Morris International (PMI), 'Glo' from British American Tobacco), carbon (*i.e.* 'CHTP' from PMI, 'Eclipse' from RJ Reynolds Tobacco Company (RJR)), and liquid fuel (*i.e.* 'Ploom' from Ploom Tech) heating systems.[5,6] The electric-heating system seems to be the most popular HNB tobacco product due to its modern appearance and the lowest amount of pollutants in smoke. Unfortunately, an electric HNB tobacco looks far from conventional cigarettes and is not sure to be widely accepted by conventional cigarette smokers. Moreover, an electric HNB product usually involves an extra charger and plug, which is not convenient for outdoor use because of its poor portability.[7] By contrast, for a carbon HNB tobacco product, the carbon fuel and tobacco are capsuled by a stick-shaped paper, making the carbon HNB product look more like a conventional smoking cigarette, which allows the smokers not to change their habits. Hence, the carbon HNB tobacco product aims for the niche between conventional and electric cigarettes,[3,8] and the carbon heating sources are receiving increasing attention from the researchers.

Generally, a carbon heating source requires good ignition performance, good thermal conductivity, and persistent burning without harmful emissions. So far, few papers have been found closely related to the research on carbon heating source for HNB products, probably because many research works are funded by the manufacturers, and most HNB manufacturers do not always report their findings in peer-reviewed journals. Fortunately, there are quite a few public patents that can hint at the research trend of the external

[a]*China Tobacco Hubei Industry Co. Ltd, Wuhan 430040, China*
[b]*State Key Laboratory of Coal Combustion, School of Energy and Power Engineering, Huazhong University of Science and Technology, Wuhan 430074, China*
[c]*School of Mechanical Engineering, Wuhan Polytechnic University, Wuhan 430048, China. E-mail: wangzean@whpu.edu.cn*

heating sources in some tobacco companies. For instance, PMI submitted several patents using carbon-based heating sources, *i.e.* ligno-cellulosic materials,[9] active carbon impregnated with transition metals, and sulfur and nitrogen ligation.[10] Meanwhile, RJR proposed a carbon-containing fuel for use in HNB tobacco,[11] graphite mixed with a metal-containing catalyst (*i.e.* $Fe(NO_3)_3$, $Cu(NO_3)_2$, $Mn(NO_3)_2$, $Zn(NO_3)_2$, *etc.*).[12] Through the comparison among different carbon sources (*i.e.* activated carbon and ligno-cellulosic material), graphite is a promising and clean carbon source with better thermal conductivity, higher calorific value, and longer combustion duration. However, graphite is not easy to be ignited by a lighter, and it seems very promising if safe and efficient additives can be found to improve the ignition performance of graphite.

Currently, plenty of chemicals (*i.e.* La_2O_3, $Ca(H_2PO_4)_2$, and CeO_2) have been used to improve combustion or as additives to upgrade the quality of fuels, including coal,[13] biomass,[14] and biodiesel.[15] However, most of them cannot act as the combustion improver of carbon HNB tobacco due to their harmfulness. Among the non-harmful combustion improvers, sodium (*i.e.* $Na_3C_6H_5O_7$, NaCl, *etc.*) and potassium salts (*i.e.* $K_3C_6H_5O_7$, K_2CO_3, *etc.*) exhibit good promotion performance,[16] which have been used as combustion improvers of cigarette papers. Moreover, potassium salts are found to be more effective in reducing the amount of smoking tar than sodium salts.[17] Hence, a potassium salt could be a better combustion improver in comparison with a sodium salt. However, the performances of different potassium additives (including organic and inorganic ones) on graphite combustion require further evaluation, and their promotion mechanisms are also unknown. Moreover, the addition amount of target potassium salt requires further evaluation and optimization.

This work aims to investigate the performances of varying potassium salts (*i.e.* $K_3C_6H_5O_7$, $KC_4H_5O_5$, $K_2C_4H_4O_6$, KOH, KNO_3, K_2CO_3, *etc.*) on graphite combustion and their promotion mechanisms. Graphite is blended with these potassium salts, and the combustion characteristics (*i.e.* ignition temperature and activation energy) are investigated by thermal gravimetric (TG) analysis. The dispersion of potassium in graphite is characterized by scanning electron microscopy (SEM) coupled with energy dispersive spectrometry (EDS), and the low-temperature ash (LTA) of the graphite is analyzed by powder X-ray diffraction (XRD). The obtained results can provide experimental support for the preparation of a carbon heating source in HNB tobacco products.

Experimental

Material and methods

Material preparation. The commercial graphite powder was sieved to 200 mesh (<75 μm) and stored in a dry sealed container for subsequent analysis and utilization. Six types of potassium salts, namely KNO_3, KOH, K_2CO_3, $K_2C_4H_4O_6$, $K_3C_6H_5O_7$, and $KC_4H_5O_5$, were used as combustion improvers. To achieve adequate mixing, graphite and potassium salts were mixed in ethanol solution due to the poor wettability of graphite in water. Potassium salts (0.03 g) and graphite powder (2.97 g) were mixed with 20 mL ethanol solution (50% in volume) to form the suspensions, which were stirred for 1 h and dehydrated at 105 °C for 8 h to obtain graphite blended with 1.00% K salts. The samples were named as given in Table 1, where 1.00% of various K additives were respectively mixed with 99.00% pure graphite to form G1 to G7. G2 sample was separately mixed with 0.30%, 0.50%, and 0.70% of K additives to generate G2-L, G2-M, and G2-H, wherein "-L", "-M", and "-H" correspond to the potassium addition amount of 0.30%, 0.50%, and 0.70%, respectively. Notably, the KNO_3 additive was only tested for performance comparison, which was excluded from subsequent mechanism investigation due to its possible release of hazardous emissions like nitrogen oxides. The LTA of the graphite samples were prepared under air atmosphere at 620 °C, which was determined according to the ignition temperature obtained from the TG-DSC curves.

TG-DSC analysis

To analyze the combustion characteristics of the graphite blended with various potassium salts, TG analysis was carried out using a simultaneous NETZSCH instrument (STA 449F3, D. E.). Finely ground sample (10 mg) was placed in a platinum crucible and was heated from room temperature to 1000 °C at 10 °C min^{-1} in flowing air of 100 mL min^{-1}. The weight loss curve of each sample was recorded by the TG analyzer. Differential Scanning Calorimetric (DSC) curves were simultaneously collected by an online computer and data processing system.

XRD and SEM-EDS

The graphite samples were analyzed by powder XRD on an automated diffractometer (D8 Advance, Bruker, D.E.) using Cu-Kα_1 radiation at 40 kV and 30 mA over 10° to 80° (2θ angle) at a rate of 5° min^{-1} to identify the mineral compositions. SEM was conducted on a scanning electron microscope (SU 8010, Hitachi, J.P.) equipped with an EDS analyzer using an

Table 1 The amounts of the improver and sample naming

Sample	Combustion improver	Fraction in weight	K mass fraction
G1	Graphite	0.00%	0.00%
G2	Graphite + potassium citrate	1.00%	0.38%
G2-L		0.78%	0.30%
G2-M		1.31%	0.50%
G2-H		1.83%	0.70%
G3	Graphite + potassium malate	1.00%	0.23%
G3-M		2.20%	0.50%
G4	Graphite + potassium tartrate	1.00%	0.35%
G5	Graphite + potassium hydroxide	1.00%	0.70%
G6	Graphite + potassium nitrate	1.00%	0.39%
G7	Graphite + potassium carbonate	1.00%	0.57%
G7-L		0.53%	0.30%
G7-M		0.88%	0.50%
G7-H		1.24%	0.70%

accelerating voltage of 15 kV. All the homogenized samples were coated with platinum to facilitate SEM observation.

Results and discussion

Thermal analysis of the samples

XRD was used to characterize the K compounds in the graphite samples, and Fig. 1 presents the XRD patterns of G1, G2, and G7. However, the K-related compounds were difficult to be uncovered in G2 and G7 samples, clearly because the K compound accounts for only 1.00% of the mixtures. Subsequently, EDS analysis results are provided in Fig. 2 to study the elemental distribution of the mixtures, where graph e/h, d/i, and e/j separately correspond to the surface distribution of the C, K, and O elements. It can be easily found that the area where K and O appear basically coincides with the area where C appears, demonstrating that the potassium compounds have been fully mixed with graphite, and the uniform distribution of C, K, and O enables the smooth proceeding of the catalytic combustion process.

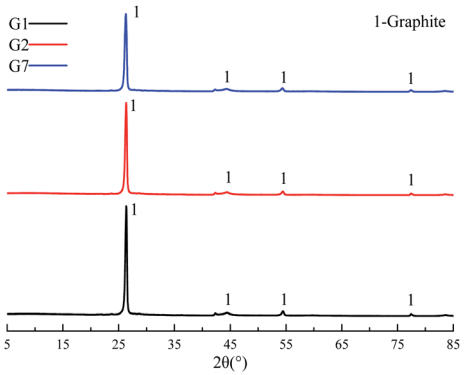

Fig. 1 XRD patterns of different graphite samples.

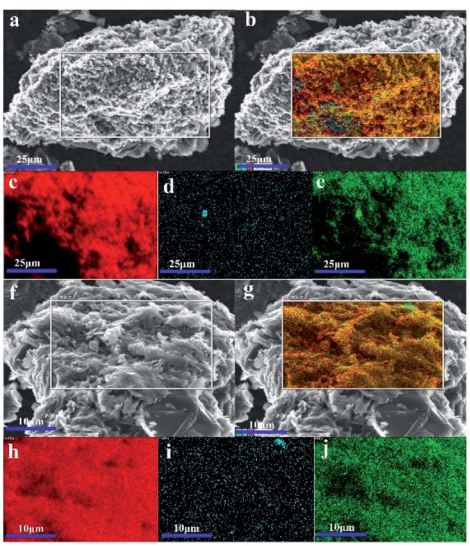

Fig. 2 EDS analysis of G2 (a–e) and G7 (f–j).

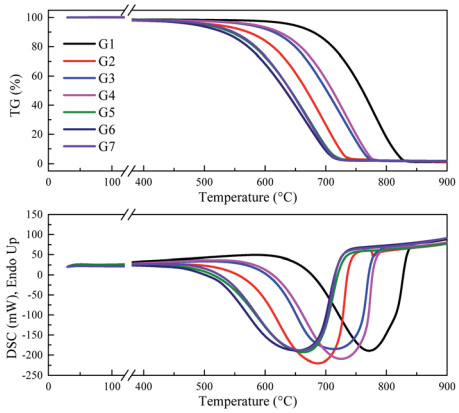

Fig. 3 TG-DSC curves of the samples, G1 to G7.

Table 2 $T_{ignition}$, T_{max}, and $T_{burnout}$ of the samples

Sample	G1	G2	G3	G4	G5	G6	G7
$T_{ignition}$ (°C)	704	612	645	654	589	580	589
T_{max} (°C)	782	685	716	730	667	655	666
$T_{burnout}$ (°C)	819	730	763	772	707	698	706

Fig. 3 displays the TG and DSC curves of graphite and the mixtures. Obviously, the samples doped with different additives exhibit very similar weight loss and exothermic profiles to those of the pure graphite sample G1. To facilitate understanding, the ignition ($T_{ignition}$) and burnout temperature ($T_{burnout}$), as well as the temperature of maximum weight loss rate (T_{max}) are summarized in Table 2 to evaluate the performance of different combustion improvers. Generally, the $T_{ignition}$, $T_{burnout}$, and T_{max} all decreased after the addition of potassium salts. Among all the additives, G1 shows the highest $T_{ignition}$ of 704 °C, indicating that pure graphite is the most difficult to be directly fired, and a necessary catalyst is required. Notably, the $K_2C_4H_4O_6$ sample possesses the highest $T_{ignition}$, $T_{burnout}$, and T_{max}, and the KNO_3 sample exhibits the highest performance. Moreover, the temperatures of G5, G6, and G7 decreased much more than those of G2, G3, and G4, clearly illustrating that inorganic K salts can favor the combustion process much more than the

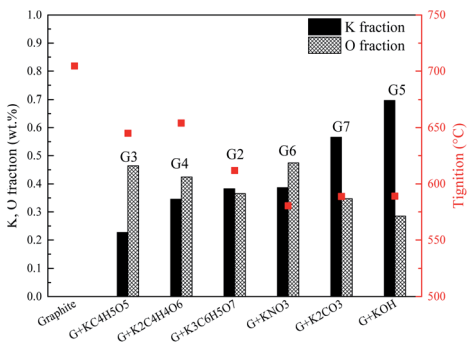

Fig. 4 Correlations between $T_{ignition}$ and K, O fractions of G1-G7.

organic K compounds. The detailed mechanism will be discussed later.

Effects of potassium/oxygen on the combustion characteristics of graphite

The promotion effects are closely related to the kind of organic/inorganic compounds, which might be associated with the potassium/oxygen content of the compounds. Therefore, the roles of K and O must be further studied to gain insight into the mechanism. To investigate the roles of K and O elements in the combustion, Fig. 4 presents the correlations between T_{max} and K, O contents. All the samples are sequenced in ascending order of the K mass fraction. Generally, $T_{ignition}$ decreases with increasing K mass fraction. When the oxygen fraction is almost the same, the additive with a higher K content definitely possesses a lower $T_{ignition}$ value. Surprisingly, the two additives $KC_4H_5O_5$ and $K_2C_2H_4O_6$ exhibit obviously different kinetics: $T_{ignition}$ is increased by 9 °C when the K fraction is elevated from 0.23% to 0.35%, probably indicating that the O element can promote the combustion process. Moreover, the $T_{ignition}$ of KNO_3 is 30 °C lower than that of $K_3C_6H_5O_7$ though they possess a very close K mass fraction, further illustrating the important role of O during catalytic combustion.

Interestingly, inorganic K additives have significant advantages over organic salts in catalytic combustion, which might be associated with the oxygen species of various K compounds. To further investigate the roles of K and O elements during catalytic combustion, Fig. 5 presents the TG and DSC curves of the graphite samples with several fixed K fractions. Organic $K_3C_6H_5O_7$, $KC_4H_5O_5$, and inorganic K_2CO_3 are selected as the additives due to their relatively high performances.

Fig. 6 displays the correlations between the $T_{ignition}$ and K, O fraction of the samples. When graphite is blended with the same additive at different addition amounts, a higher K addition amount undoubtedly corresponds to a lower $T_{ignition}$. Notably, with the $K_3C_6H_5O_7$ additive, the $T_{ignition}$ decreased by 24 °C from 617 to 593 °C with an increase in the K fraction from 0.30% to 0.50%, while the $T_{ignition}$ only reduced by 4 °C from 593 to 589 °C when the K fraction was continuously elevated from 0.50% to 0.70%, and a similar phenomenon is observed for

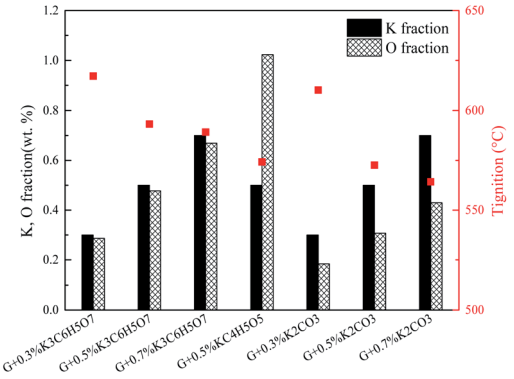

Fig. 6 Correlations between $T_{ignition}$ and K, O fraction (G2-L, G2-M, G2-H, G5, G7-L, G7-M, and G7-H).

K_2CO_3 additive. Therefore, the decline of $T_{ignition}$ does not seem to be proportional to the K fraction increase, probably suggesting that the continuous increase of K amount does not always reduce the ignition temperature if the amount of K additive exceeds the threshold value. Fig. 7 summarizes the ignition temperature of the graphite samples. For the K_2CO_3 additive, when the K fraction content is elevated from 0.50% to 0.70%, the ignition temperature declined by only 10 °C. Moreover, when the K fractions are equal to 0.50%, the ignition temperature of different samples (G2-M, G3-M, and G7-M) does not simply decrease as the oxygen content increases, suggesting that the effect of oxygen in the catalytic combustion process is very complicated. It could be figured out by the assumption below: K can play the role of "O_2 transfer" in the catalytic combustion.[18] Covalently bound K and O (K_2CO_3) can react with atmospheric O_2 on the carbon surface to form the active intermediate K_2O_2, which is produced due to the breaking of the K–O bond in K_2CO_3.[19,20] The active intermediate K_2O_2 can catalytically oxidize graphite carbon to generate K_2O and CO_2.[21] Subsequently, K_2O can further react with atmospheric O_2 to form K_2O_2, thereby providing K_2O_2 for the next stage graphite oxidation, which can be described by eqn (1)–(4). At the initial stage, atomic O in the additives could combine with potassium compounds to produce K_2O_2, while it is not easy for the organic O to combine with K since the organic carbocyclic O is much more stable than inorganic O, and it would take more energy

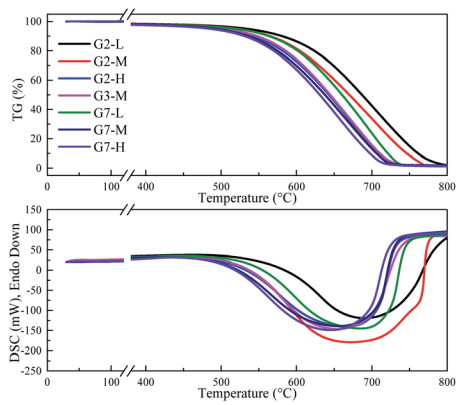

Fig. 5 TG-DSC curves for the graphite samples.

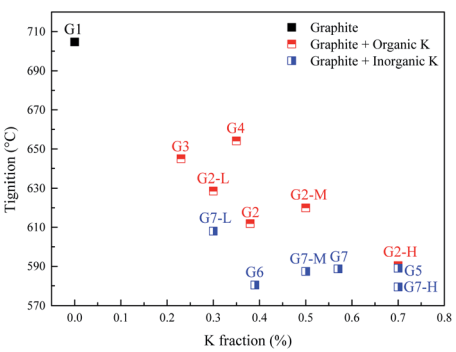

Fig. 7 $T_{ignition}$ of graphite samples with varying additives.

(heat) to break the carbon ring structure. As a result, the ignition temperature with inorganic potassium is usually lower than that with an organic potassium additive.

$$K_2CO_3 + \tfrac{1}{2}O_2 \rightarrow K_2O_2 + CO_2 \quad (1)$$

$$2K_2O_2 + C \rightarrow 2K_2O + CO_2 \quad (2)$$

$$K_2O + \tfrac{1}{2}O_2 \rightarrow K_2O_2 \quad (3)$$

$$K_2O + CO_2 \rightarrow K_2CO_3 \quad (4)$$

Fig. 8 shows the SEM images of LTA of G1, G2-M, and G7-M. Once the samples are heated to 620 °C, G2-M and G7-M can be ignited but not graphite. In Fig. 8a and b, the unburned graphite presents a layered and dense structure, which has not been damaged by the heating process. Simultaneously, G2-M in Fig. 8c and d exhibits a granular and loose structure, indicating that the structure of the edge is gradually destroyed in the combustion process at 620 °C. Fig. 8e and f displays a cottony and curled structure, which is even fading to white, clearly showing the combustion process with the K additive, and G7-M is burned more completely than G2-M.

Kinetic analysis for the combustion process

Combined with the experimental data, reaction kinetics are conducted to gain insight into the underlying mechanisms of the combustion process with different potassium additives. A chemical reaction mechanism function in eqn (5) can be used to describe the weight loss process of the graphite.

$$f(\alpha) = (1 - \alpha)^n \quad (5)$$

$$\alpha = \frac{W_t - W_0}{W_\infty - W_0} \quad (6)$$

where α is the conversion ratio of the graphite and n stands for the order of the reaction; W_0, W_t, and W_∞ respectively represent the sample weight at the initial time, time t, and the termination time, g.

For a slow heating combustion process, the reaction rate is considered to be controlled by chemical kinetics, and the relationship between the reaction rate and temperature follows the Arrhenius law in eqn (7).

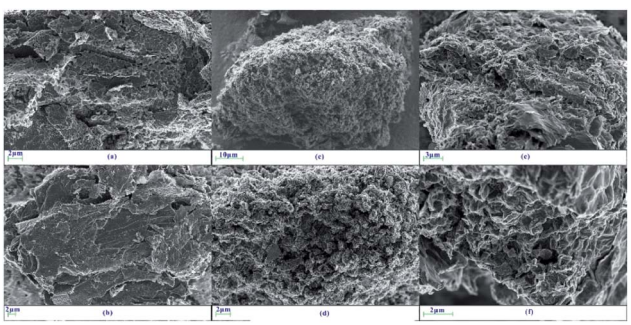

Fig. 8 SEM images of the graphite (a and b), G2-M (c and d), and G7-M (e and f).

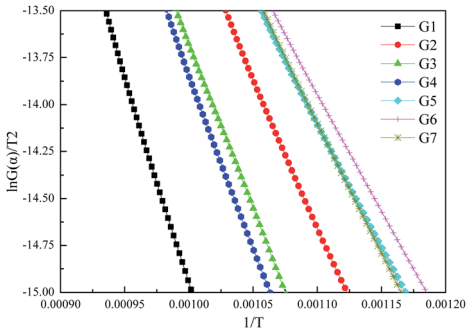

Fig. 9 Linear regression results of the graphite samples.

$$\frac{d\alpha}{dt} = \frac{A}{\beta}\exp\left(-\frac{E}{RT}\right)f(\alpha) \quad (7)$$

where A is the pre-exponential factor, min^{-1}; β is the heating rate, 10 K min^{-1}; E is the activation energy, kJ mol^{-1}; R is the universal gas constant, 8.314 × 10^{-3} kJ mol^{-1} K^{-1}; T is the temperature in Kelvin.

Eqn (7) is then processed by using Coats–Redfern method,[22] and eqn (8) is obtained for convenient data fitting, where $G(\alpha)$ is determined by integrating the formula in eqn (9). The values of $-(E/R)$ and $\ln(AR/\beta E)$ are obtained from the slope and the intercept of the straight-lines from the linear regression of $\ln(G(\alpha)/T^2)$ against $1/T$. $G(\alpha)$ should be $-\ln(1 - \alpha)$ for a first-order kinetic model, which is generally suitable to describe the combustion of coal or biomass.

$$\ln\frac{G(\alpha)}{T^2} = \ln\frac{AR}{\beta E} - \frac{E}{RT} \quad (8)$$

$$G(\alpha) = \int_0^\alpha \frac{d\alpha}{f(\alpha)} \quad (9)$$

Fig. 9 displays the linear regression results of $\ln(G(\alpha)/T^2)$ against $1/T$, and corresponding parameters are summarized in Table 3. The values of R^2 indicate that the first-order kinetic model can well depict the combustion process of graphite.

Combustion of G1 requires the maximum E value of 194.5 kJ mol^{-1}, and G6 combustion needs the smallest E of 106.8 kJ mol^{-1}. After the addition of K salts, the activation energy required for combustion sharply reduced from 194.5 to 106.8 kJ mol^{-1}, making the occurrence of reaction much easier.

Table 3 Regression results of the graphite samples

Sample	Slope	Intercept	R^2	E (kJ mol^{-1})	A (min^{-1})
G1	−23390	8.4247	0.996	194.5	1.07×10^9
G2	−15606	2.5254	0.999	129.7	1.95×10^6
G3	−17480	3.8289	0.998	145.3	8.04×10^6
G4	−17650	3.8263	0.996	146.7	8.10×10^6
G5	−13410	0.675	0.998	111.5	2.63×10^5
G6	−12846	0.2128	0.998	106.8	1.59×10^5
G7	−14050	1.3776	0.999	116.8	5.57×10^5

Conclusions

The effects of various potassium salts on the combustion characteristics of graphite are investigated in the current work, and the conclusions are summarized as follows: (1) the ignition temperature of graphite can be decreased from 705 to 580 °C after the addition of KNO_3, and the promotion effect can be sequenced as KNO_3 > K_2CO_3 > KOH > $K_3C_6H_5O_7$ > $KC_4H_5O_5$ > $K_2C_4H_4O_6$. Further kinetic analysis indicates that the addition of potassium salts can significantly reduce the activation energy by 50–85 kJ mol^{-1}; (2) the ignition temperature is decreased with increasing K amount because K plays a role like "O_2 transfer": K can interact with oxygen on the graphite surface and transfer atmospheric O_2 to produce K_2O_2, which can support the catalytic combustion process. However, the ignition temperature does not always decline with increasing O content because potassium takes more energy to react with an organic carbocyclic O than an inorganic O atom to generate the initial intermediates. Hence, inorganic potassium salts with higher K, O mass fraction should be better choices; (3) among all the tested K additives, K_2CO_3 is a suitable catalyst for graphite combustion, and the addition amount is around 0.88% in weight (K mass fraction = 0.50%).

Author contributions

Chenghao Luo: writing – original draft; Dan Li: investigation; Long Huang: resources & funding acquisition; Zean Wang: writing – review & editing & formal analysis; Jian Zhang: methodology & data curation; Hao Liu: conceptualization & project administration; Zhaohui Liu: supervision;

Conflicts of interest

There are no conflicts to declare.

Acknowledgements

The authors acknowledge the support of the China Tobacco Hubei Industry Co. Ltd. and Innovation Research Foundation of Huazhong University of Science and Technology (Grant No. 5001120031).

Notes and references

1 C. A. Gehrman and M. F. Hovell, *Nicotine Tob. Res.*, 2003, **5**, 289–301.
2 E. Simonavicius, A. McNeill, L. Shahab and L. S. Brose, *Tob. Control*, 2019, **28**, 582.
3 T. L. Caputi, *Tob. Control*, 2016, **26**, 609–610.
4 L. Frank, H. Christelle, W. Rolf and M. John, *Nicotine Tob. Res.*, 2016, 1606–1613.
5 C. K. Banerjee, D. C. Kay and R. L. Lehman, *US Pat.*, US4827950, 1989.
6 R. N. Batista, *US Pat.*, US10111463, 2018.
7 H. Xu, Y. Chen and J. G. Tang, *J. Anhui Agric. Sci.*, 2017, **45**, 3.
8 M. R. Smith, B. Clark, F. Lüdicke, J. P. Schaller, P. Vanscheeuwijck, J. Hoeng and M. C. Peitsch, *Regul. Toxicol. Pharmacol.*, 2016, **81**, S17–S26.
9 J. R. Hearn, V. Lanzillotti and G. H. Burnett, *US Pat.*, US5060676, 1991.
10 J. B. Paine, *US Pat.*, US6789547 B1, 2004.
11 E. G. Farrier, J. L. White, *Europa Pat.*, EP0236992, 1991.
12 C. K. Banerjee and S. B. Sears, *US Pat.*, US8469035, 2008.
13 Y. Sun, B. Hu, Q. Lü and S. Zhang, *Int. J. Coal Sci. Technol.*, 2016, **3**, 47–52.
14 Q. Wang, K. Han, J. Gao, H. Li and C. Lu, *Fuel*, 2017, **199**, 488–496.
15 H. Jung, D. B. Kittelson and M. R. Zachariah, *Combust. Flame*, 2005, **142**, 276–288.
16 H. R. Li, Y. Liu, D. Li, B. Cai and Z. G. Cheng, *Chin. J. Chem.*, 2010, **28**, 1322–1326.
17 Z. Liu, C. Ling, M. Miao, Z. Zhu and H. U. Qun, *Tob. Sci. Technol.*, 2017, **50**, 93–102.
18 M. Zevenhoven, C. Sevonius, P. Salminen, D. Lindberg, A. Brink, P. Yrjas and L. Hupa, *Energy*, 2018, **148**, 930–940.
19 J. M. Saber, K. B. Kester, J. L. Falconer and L. F. Brown, *J. Catal.*, 1988, **109**, 329–346.
20 W. Teus, E. Rien and J. A. Moulijn, *Carbon*, 1983, **21**, 1–12.
21 H. Zhu, X. Wang, J. Zhang, K. Yao, G. Yu and X. Wang, *Energy Technol.*, 2015, **3**, 961–967.
22 A. W. Coats and J. P. Redfern, *Nature*, 1964, **201**, 68–69.